On the need of individually optimizing temporal interference stimulation of human brains due to inter-individual variability

Tapasi Brahma[1], Alexander Guillen[1], Abhishek Datta[1,2], Yu Huang[1]

[1] Soterix Medical Inc., Woodbridge, NJ 07095
[2] The City College of New York, New York, NY 10031

Abstract

Transcranial temporal interference stimulation (TI, TIS, or tTIS), also known as interferential stimulation (IFS), is able to focally stimulate deep brain regions, provided it is properly optimized. We previously presented an algorithm for optimizing TI using two arrays of electrodes and showed that it can achieve more focal stimulation compared to optimized high-definition transcranial electrical stimulation (HD-TES) and conventional optimized TI using two pairs of electrodes, especially in the deep brain areas such as the hippocampus. However, those modeling studies were only performed on an averaged head (MNI152 template) along with three individual heads. Existing TI work in the literature mostly does not optimize the stimulation but only utilizes a common (possibly optimized) montage of two pairs of electrodes on different individual heads. Here we aim to study the inter-individual variability of optimized TI by applying the same optimization algorithms on N = 10 heads using their individualized head models. Specifically, we compared the focality achieved by different stimulation techniques at three different regions of interest (ROI; right hippocampus, left dorsolateral prefrontal cortex, and left motor cortex). As expected, there is a variability in focality achieved by TI of up to 0.95 cm at the same ROI across subjects due to inter-individual differences in the head anatomy and tissue conductivity. Again we show that optimized TI using two arrays of electrodes achieve higher focality compared to optimized HD-TES at the same level of modulation intensity, especially at the deep brain locations. Compared to using a common montage obtained from a standard head (MNI152 template), individually optimized HD-TES does not significantly improve the stimulation focality at the ROIs. However, individually optimized TI does significantly improve the focality by up to ~4 cm for TI using two pairs of electrodes, and by up to ~1 cm for TI using two arrays of electrodes. This work demonstrates the need of individually optimizing TI to target deep brain areas, and advocates against using a common head model and montage for TI modeling and experimental studies.

Introduction

Transcranial electrical stimulation (TES) delivers weak electric current (≤ 2 mA) to the scalp in order to modulate neural activity of the brain (Nitsche and Paulus, 2000). TES has been shown to improve cognitive functions and help treat some neurological diseases such as major depression (Bikson et al., 2008), epilepsy (Auvichayapat et al., 2013; Fregni et al., 2006b), Parkinson's disease (Fregni et al., 2006a), chronic pain (Fregni et al., 2007), and stroke (Meinzer et al., 2016). Conventional TES using two sponge electrodes is shown to generate diffused electric fields and cannot reach deep targets in the brain (Datta et al., 2009). High-definition TES (Datta et al., 2009; Edwards et al., 2013) utilizing several small disc electrodes has thus been proposed to achieve more focal or more intense stimulation. Several algorithms have been developed along this line for optimizing HD-TES in terms of focality or intensity of the induced electric field (Dmochowski et al., 2011; Guler et al., 2016; Huang et al., 2018; Ruffini et al., 2014;

Sadleir et al., 2012). However, even with optimized stimulation montages, modeling studies have shown that HD-TES is not able to focally stimulate deep brain regions (Dmochowski et al., 2011; Huang and Parra, 2019).

Recently transcranial temporal interference stimulation (TI, TIS, or tTIS), also known as interferential stimulation (IFS), has drawn much attention in the TES community as both computational and experimental studies show that TI can reach deep brain areas (Grossman et al., 2017; Huang et al., 2020; Huang and Datta, 2021; Violante et al., 2023). TI applies sinusoidal waveforms of similar frequency through two pairs of electrodes. The resulting interfered electric field is thus amplitude modulated containing both a fast oscillating carrier signal in the kHz range and a slowly oscillating modulation envelope in the low frequency range. The premise of TI is that neurons only respond to the slower oscillation due to their property of low-pass filtering (Grossman et al., 2017). Computational researchers have since been working on optimizing the placement of the two pairs of electrodes on the scalp to maximize stimulation focality. Most of these efforts are considering only two pairs of electrodes as originally proposed by Grossman et al (Lee et al., 2020; Rampersad et al., 2019; von Conta et al., 2021). Some are trying to extend to multiple (>2) pairs of electrodes but the underlying algorithms are either *ad hoc* (Lee et al., 2022), or not systematically optimizing the electrode locations (Xiao et al., 2019) or the full physics of TI (Cao and Grover, 2020). To the best of our knowledge, we are the first to formulate a rigorous mathematical framework to optimize the full physics of the interfered envelope of TI based on two arrays of multi-channel electrodes (up to 93 per frequency) instead of two pairs or multi pairs of electrodes (Huang et al., 2020). We showed *in silico* that compared to HD-TES, optimized multi-channel TI stimulates deep brain areas with much higher focality at the same modulation strength (Huang et al., 2020). We further showed that compared to optimized TI using two pairs of electrodes, optimized multi-channel TI also shows higher focality at the same modulation strength (Huang and Datta, 2021).

However, we only tested our optimization algorithms for TI on the averaged standard head (Huang et al., 2020) and up to three individual heads (Huang and Datta, 2021). Considering inter-individual variability in head anatomy (Datta et al., 2012) and tissue conductivity (Huang et al., 2017), we expect to see differences across subjects in the optimal montages for stimulating the same target location in the brain. Existing computational and experimental work in the literature mostly use a common head model or electrode montage to study TI (Grossman et al., 2017; Vassiliadis et al., 2024; Violante et al., 2023). This may explain why TI did not show any effect when applied on the visual cortex of 10 subjects in a recent work (Iszak et al., 2023). In this paper we show that (1) optimal TI montages vary significantly across subjects; (2) optimized TI always show higher focality compared to optimized HD-TES; and (3) a common montage always gives worse focality under TI stimulation compared to individually optimized ones, no matter whether two pairs of electrodes or two arrays of electrodes are used. We therefore argue that individualized modeling and optimization is important in future TI studies.

Materials and Methods

Individualized head models

Ten individual T1-weighted magnetic resonance images (MRI) were randomly selected from the 1200 Subjects Data Release in the Human Connectome Project (Van Essen et al., 2012). Open-source toolbox ROAST (Huang et al., 2019) was used on each of these subjects to generate individualized lead-field that is needed for optimized HD-TES (Dmochowski et al., 2011) and

optimized TI (Huang et al., 2020; Huang and Datta, 2021). Specifically, with a simple one-line command (Huang, 2019), ROAST segmented out six tissues in the individual head MRI (gray matter, white matter, cerebrospinal fluid, skull, scalp, air cavities), placed 72 high-definition disc electrodes following the international 10/10 system (Klem et al., 1999) on the scalp surface, and generated the lead field for each of the electrodes with Iz as the cathode.

Optimization of HD-TES and TI

We used existing algorithms (Dmochowski et al., 2011; Huang et al., 2020; Huang and Datta, 2021) for optimizing HD-TES and TI to stimulate 3 target locations in the brain: right hippocampus (MNI coordinates [28,-22,-14]), left dorsolateral prefrontal cortex (DLPFC, MNI coordinates [-39,34,37]), and left motor cortex (MNI coordinates [-48,-8,50]). These MNI coordinates were mapped into each individual head using the transform estimated by the segmentation algorithm utilized by ROAST (Ashburner and Friston, 2005; Huang et al., 2019). We solved the optimization for 2-array TI and HD-TES at the same time. Specifically, we initialized the optimization for 2-array TI using solutions from max-focality HD-TES at the same target location, and varied the energy constraints at non-target areas for 12 different levels (Huang et al., 2020). For safety consideration, the total injected current was limited to 2 mA. For 2-pair TI optimization, we performed an exhaustive search to find the best two pairs of electrodes that achieves the highest focality of modulation at the target. Here focality was defined as the size of the brain volume stimulated at 50% (or more) of the modulation at the target (similar to the concept of full width at half maximum (FWHM) in classic imaging (Gonzalez and Woods, 2002)). Specifically, the search was performed across: (1) four possible electrodes selected from the 72 placed electrodes on the scalp; (2) three possible ways of pairing in these four electrodes for the two frequencies used in TI; (3) amplitudes of injected current at one pair of electrodes, in the range of 0.5 mA to 1.5 mA, with a step size of 0.05 mA and the sum across the two pairs of electrodes being 2 mA. In total 64,813,770 montages were considered for one target in the head model (1,028,790 possible combinations of 4 electrodes × 3 possible ways of pairing × 21 amplitudes of injected current, Huang and Datta, 2021). Note for all optimization problems, we optimized the modulation depth along the radial direction, i.e., the direction pointing from the target location to the center of the brain (defined as MNI coordinates of [0,0,0]). The modulation depth is the strength of the envelope of the interfered signal from the two pairs (or arrays) of electrodes. For more technical details, one is referred to Huang, 2023; Huang et al., 2020; Huang and Datta, 2021; Huang and Parra, 2019.

Comparison between optimized HD-TES and optimized TI

Different levels of energy constraints at the non-target areas give different optimal electrode montages, as represented by a focality-modulation curve (Huang et al., 2020). Solutions under very strict (i.e., small) energy constraints usually result in electrode montages that do not use up all the 2 mA budget of injected current (Huang et al., 2020). We therefore discarded these solutions when analyzing the results. When showing examples of electrode montages across subjects and stimulation modalities (HD-TES and 2-array TI), we used the strictest energy constraint at which the injected current just reaches the total budget of 2 mA, i.e., the left-most point on the focality-modulation curve. Note that at the same level of energy constraint, HD-TES and 2-array TI may not return the same modulation depth. To facilitate comparison of focalities between these two stimulation modalities, we made sure that HD-TES outputs the same modulation at the target as that from 2-array TI by fine-tuning the energy constraint for HD-TES.

As we will see in the Results section, the focality-modulation curve spans for different subjects at different locations in the focality-modulation space. To facilitate comparison across subjects and stimulation modalities, we mapped the curve for each subject to a normalized modulation depth between 0% and 100% by linear interpolation. Note for 2-pair TI, no energy constraint was explicitly specified in the searching algorithm, so the optimal montage is unique for a specific target on a specific subject.

Comparison of optimized vs. common montages

To show the performance of using a common montage on individual heads compared to that of using individually optimized montages, we also computed the optimal montages of HD-TES, 2-array TI, and 2-pair TI on the MNI152 head (Grabner et al., 2006). We then applied these optimal montages from the MNI152 head (i.e., common montages) onto the ten individual heads, computed the achieved stimulation focality at the 3 targets, and compared them to those from using individually optimized montages. Note that for HD-TES and 2-array TI, we again calculated the results for 12 different levels of energy constraints, and performed the same normalization process on the modulation depth to facilitate the comparison. For 2-pair TI there is only one unique solution for a specific target on a specific head.

Results

Inter-individual variability of optimized TI and HD-TES

(Fig. 1 to be here)

Fig. 1 shows the optimized montages for targeting the right hippocampus in the first five subjects, at the smallest energy constraint where the injected current just reaches 2mA. The left column (A1-E1), middle column (A2-E2), and right column (A3-E3) shows the optimized montages from conventional HD-TES, 2-array TI, and 2-pair TI, respectively. It is evident that the optimal montages vary significantly across different subjects for targeting the same location in the brain, for all the three stimulation modalities, due to inter-individual variabilities in head anatomy and tissue conductivity. We note some interesting patterns on the spatial distribution of stimulation electrodes for the 2-array TI: one frequency tend to concentrate on the right scalp (panels A2–E2, right topoplots), and for the 2-pair TI, the two frequencies are separated at the left and right scalps, with the locations of the electrodes on the left scalp changing significantly across subjects (panels A3–E3). We found similar patterns on the other five subjects.
The standard deviation of these injected current across the ten subjects at each electrode is shown in Fig. 2, for the three target locations: right hippocampus (row A1-A3), left DLPFC (row B1-B3), left motor cortex (row C1-C3), and the three stimulation modalities: conventional HD-TES (column A1-C1), 2-array TI (column A2-C2), 2-pair TI (column A3-C3). Note that the maximal standard deviation is 0.99 mA (panel C3).

(Fig. 2 to be here)

The inter-individual variability can also be seen in the focality-modulation curves shown in Fig. 3. Different subjects have the curves residing in different locations in the focality-modulation plane. For the sake of comparison across subjects, we normalized the modulation depth into the range of 0% and 100% by linear interpolation. We see that under the same level of modulation

depth, the focality at the target varies across subjects. For example, at the normalized modulation depth of 80%, focality of HD-TES has a standard deviation of 0.32 cm for Target 1 (Fig. 3B1, blue shaded curve), 0.53 cm for Target 2 (Fig. 3B2), and 0.98 cm for Target 3 (Fig. 3B3). For 2-array TI, this standard deviation is 0.26 cm (Fig. 3B1, red shaded curve), 0.55 cm, and 0.92 cm for the three targets, respectively. For 2-pair TI, this standard deviation is 0.27 cm (Fig. 7A1, circles), 0.59 cm (Fig. 7A2), and 0.95 cm (Fig. 7A3) for the three targets, respectively.

(Fig. 3 to be here)

Optimized 2-array TI achieves higher focality than optimized HD-TES in all individuals

At the same level of modulation depth, optimized 2-array TI and optimized HD-TES achieve different focalities, for all the ten individual heads (Fig. 3). A two-way (modulation, method) repeated measures ANOVA shows that this difference between TI and HD-tES is significant (for the three targets: $F(1,63)=6.99$, $p=0.03$; $F(1,61)=25.27$, $p<0.001$; $F(1,54)=10.76$, $p=0.01$). At the 80% modulation, a pair-wise t-test shows that TI has significantly better focality than HD-tES (for the three targets: $t(9)=4.98$, $p<0.001$; $t(9)=2.84$, $p=0.02$; $t(9)=2.29$, $p=0.048$). This difference is more obvious in the deeper targets than the cortical targets, consistent with our previous finding on the MNI152 head (Huang et al., 2020).

To visualize this difference, Fig. 4 shows some examples. Fig. 4A is from Subject 3 at the 4th energy constraint for targeting the right hippocampus, Fig. 4B is from Subject 3 at the 8th energy constraint for targeting the left DLPFC, and Fig. 4C is from Subject 6 at the 9th energy constraint for targeting the left motor cortex. Here subjects and energy constraints were chosen arbitrarily to just show the examples. We slightly adjusted the energy constraint for HD-TES so that it generates the same modulation at the target as that from 2-array TI. The boost in focality in TI is more evident in the deep target than the cortical target (e.g., 2.05 cm boost in the right hippocampus (Fig. 4, panels A2&A6) vs. 0.19 cm improvement in the left motor cortex (Fig. 4, panels C2&C6), which is consistent with our previous finding on the MNI152 head (Huang et al., 2020). Note that more electrodes are needed for targeting deeper structures (Fig. 4, A1, A4, A5 vs. C1, C4, C5).

(Fig. 4 to be here)

(Fig. 5 to be here)

Individually optimized TI montages give higher focality than that from common montages

(Fig. 6 to be here)

(Fig. 7 to be here)

Fig. 5 shows the focality-modulation curves for all the ten subjects from using individually optimized montages and a common montage obtained from the standard MNI152 head targeting the three locations being studied, using conventional HD-TES. Interestingly, individually optimized and common montages do *not* give significantly different results (Fig. 5, B1–B3; two-way repeated measures ANOVA for the three targets: $F(1,63)=0.30$, $p=0.60$; $F(1,61)=1.27$, $p=0.29$; $F(1,55)=0.93$, $p=0.36$). However, this is not true for the 2-array TI, where

individually optimized montages give significantly different focalities compared to those from using a common montage (Fig. 6, B1–B3; two-way repeated measures ANOVA for the three targets: $F(1,83)=7.90$, $p=0.02$; $F(1,67)=8.60$, $p=0.02$; $F(1,57)=11.01$, $p=0.01$). At the normalized modulation depth of 80%, compared to using the individually optimized montages, using a common montage drops the focality in average 0.98 cm for Target 1, 0.50 cm for Target 2, and 0.35 cm for Target 3. A pair-wise t-test shows that this drop is significant (for the three targets: $t(9)=5.95$, $p<0.001$; $t(9)=3.07$, $p=0.01$; $t(9)=2.27$, $p=0.049$).
For the more popular 2-pair TI, we observe an even more obvious difference between using individually optimized montages and a common montage (Fig. 7). Using a common montage on individual heads without optimization leads to a significantly worse focality at the target (focality drops in average: 4.02 cm at Target 1 ($p<0.0001$); 2.92 cm at Target 2 ($p<0.001$); and 2.32 cm at Target 3 ($p<0.001$)). Note the drop is bigger in the deep location (Target 1). The common montage also generates weaker modulation strength at the target, even though not significant for the shallow location (MD drops in average: 0.03 V/m at Target 1 ($p<0.001$); 0.11 V/m at Target 2 ($p<0.0001$); and 0.04 V/m at Target 3 ($p=0.09$)). All p values are from pair-wise t-test.

(Fig. 8 to be here)

As some examples, Fig. 8 visualizes the difference between using optimized and common montages in targeting the right hippocampus, for the three stimulation modalities (HD-TES, 2-array TI, and 2-pair TI). Fig. 8A is Subject 3 at the 5th energy constraint, and Fig. 8B is Subject 3 at the 4th energy constraint. Again subjects and energy constraints were chosen arbitrarily to just show the examples. Fig. 8C is Subject 3 under TI using two pairs of electrodes. Note using common montage for TI did not output the same modulation as it was obtained from the standard MNI152 head instead of the head being studied. We noticed a small drop in focality when using a common montage for HD-TES (0.34 cm, Fig. 8, panels A5&A2), but a 10 times big drop in 2-array TI (3.40 cm, Fig. 8, panels B7&B3), and also an almost 7 times drop in 2-pair TI (2.29 cm, Fig. 8, panels C7&C3).

Discussions

TI has become a popular method for non-invasive brain stimulation recently. However, to the best of our knowledge, all the work studying inter-individual variability used a same (possibly optimized) montage across different individual heads (Acerbo et al., 2022; Hirata et al., 2024; Thiele et al., 2024; von Conta et al., 2022, 2021; Yatsuda et al., 2024; Zhang et al., 2022). This work investigated the inter-individual variability with individually optimized montage and showed *in silico* that there is substantial inter-individual variability in the optimal montages and achieved focality targeting the same brain region. The variability could be due to the differences in head anatomies and tissue conductivities across subjects (Datta et al., 2012; Huang et al., 2017). We found that using a common montage will not achieve the maximal focality or modulation strength for each subject at the target, no matter if it’s two arrays or two pairs of electrodes. The drop in focality at the target is up to 4 cm when using a common montage, comparable to the size of some regions of interest in the brain such as the pulvinar, which is a popular region to modulate in schizophrenia (Alemán-Gómez et al., 2020; Kemether et al., 2003). Therefore, adopting a common montage optimized for one head model targeting a specific region may not guarantee targeted TI stimulation of the same region on other heads, demonstrating the need to individually optimize the montages. This may also help explain why recent work showed that TI

fails to induce expected effects when no individual optimization was performed (Iszak et al., 2023).

This work also replicated on 10 more heads the previously reported superiority of optimized 2-array TI in terms of focality compared to conventional optimized HD-TES, especially in the deep brain regions (Huang et al., 2020). Note that the boost in focality from conventional HD-TES to 2-array TI in this work is less than what we previously reported in Huang et al., 2020, as in this work only 72 candidate electrodes were placed on the scalp, excluding those extra 21 electrodes placed at the lower part of the head as in Huang et al., 2020 which may help guide the current to reach the deep brain regions.

This work has some limitations. First, all the results here need to be validated by empirical recordings *in vivo*. Although there are indirect functional *in vivo* imaging on human subjects and electrical recordings on a human cadaver head (Violante et al., 2023), direct *in vivo* recordings of intracranial electrical signals during TI are still lacking in the literature. These data may help examine if the modulation depth is even the proper quantity to optimize for TI, considering its caveats reported recently (Huang, 2023; Mirzakhalili et al., 2020). Ongoing work on measuring the electrical potential under TI stimulation in a saline-filled tank shows improved focality under 6-pair TI compared to 2-pair TI (unpublished results). Further work is needed to establish the empirical evidence of the advantage in focality of using multi-channel TI. Secondly, we note that there is still no device available for 2-array TI even though the model shows that it can achieve better focality than 2-pair TI and conventional HD-TES. Ongoing work is manufacturing multi-channel (up to 32 per frequency) TI devices for 2-array TI.

Acknowledgements

This work was supported by grants from the National Institute of Health (NIH): 1R44MH126833-01A1 and Department of Education (ED): 91990022C0043.

References

Acerbo, E., Jegou, A., Luff, C., Dzialecka, P., Botzanowski, B., Missey, F., Ngom, I., Lagarde, S., Bartolomei, F., Cassara, A., Neufeld, E., Jirsa, V., Carron, R., Grossman, N., Williamson, A., 2022. Focal non-invasive deep-brain stimulation with temporal interference for the suppression of epileptic biomarkers. Front. Neurosci. 16.

Alemán-Gómez, Y., Najdenovska, E., Roine, T., Fartaria, M.J., Canales-Rodríguez, E.J., Rovó, Z., Hagmann, P., Conus, P., Do, K.Q., Klauser, P., Steullet, P., Baumann, P.S., Bach Cuadra, M., 2020. Partial-volume modeling reveals reduced gray matter in specific thalamic nuclei early in the time course of psychosis and chronic schizophrenia. Hum. Brain Mapp. 41, 4041–4061. https://doi.org/10.1002/hbm.25108

Ashburner, J., Friston, K.J., 2005. Unified segmentation. NeuroImage 26, 839–851. https://doi.org/10.1016/j.neuroimage.2005.02.018

Auvichayapat, N., Rotenberg, A., Gersner, R., Ngodklang, S., Tiamkao, S., Tassaneeyakul, W., Auvichayapat, P., 2013. Transcranial Direct Current Stimulation for Treatment of Refractory Childhood Focal Epilepsy. Brain Stimulat. 6, 696–700. https://doi.org/10.1016/j.brs.2013.01.009

Bikson, M., Bulow, P., Stiller, J., Datta, A., Battaglia, F., Karnup, S., Postolache, T., 2008. Transcranial direct current stimulation for major depression: A general system for quantifying transcranial electrotherapy dosage. Curr. Treat. Options Neurol. 10, 377–385. https://doi.org/10.1007/s11940-008-0040-y

Cao, J., Grover, P., 2020. STIMULUS: Noninvasive Dynamic Patterns of Neurostimulation Using Spatio-Temporal Interference. IEEE Trans. Biomed. Eng. 67, 726–737. https://doi.org/10.1109/TBME.2019.2919912

Datta, A., Bansal, V., Diaz, J., Patel, J., Reato, D., Bikson, M., 2009. Gyri –precise head model of transcranial DC stimulation: Improved spatial focality using a ring electrode versus conventional rectangular pad. Brain Stimulat. 2, 201–207. https://doi.org/10.1016/j.brs.2009.03.005

Datta, A., Truong, D., Minhas, P., Parra, L.C., Bikson, M., 2012. Inter-Individual Variation during Transcranial Direct Current Stimulation and Normalization of Dose Using MRI-Derived Computational Models. Front. Psychiatry Front. Res. Found. 3, 91. https://doi.org/10.3389/fpsyt.2012.00091

Dmochowski, J.P., Datta, A., Bikson, M., Su, Y., Parra, L.C., 2011. Optimized multi-electrode stimulation increases focality and intensity at target. J. Neural Eng. 8, 046011. https://doi.org/10.1088/1741-2560/8/4/046011

Edwards, D., Cortes, M., Datta, A., Minhas, P., Wassermann, E.M., Bikson, M., 2013. Physiological and modeling evidence for focal transcranial electrical brain stimulation in humans: A basis for high-definition tDCS. NeuroImage 74, 266–275. https://doi.org/10.1016/j.neuroimage.2013.01.042

Fregni, F., Boggio, P.S., Santos, M.C., Lima, M., Vieira, A.L., Rigonatti, S.P., Silva, M.T.A., Barbosa, E.R., Nitsche, M.A., Pascual-Leone, A., 2006a. Noninvasive cortical stimulation with transcranial direct current stimulation in Parkinson's disease. Mov. Disord. 21, 1693–1702. https://doi.org/10.1002/mds.21012

Fregni, F., Freedman, S., Pascual-Leone, A., 2007. Recent advances in the treatment of chronic pain with non-invasive brain stimulation techniques. Lancet Neurol. 6, 188–191. https://doi.org/10.1016/S1474-4422(07)70032-7

Fregni, F., Thome-Souza, S., Nitsche, M.A., Freedman, S.D., Valente, K.D., Pascual-Leone, A., 2006b. A Controlled Clinical Trial of Cathodal DC Polarization in Patients with Refractory Epilepsy. Epilepsia 47, 335–342. https://doi.org/10.1111/j.1528-1167.2006.00426.x

Gonzalez, R.C., Woods, R.E., 2002. Digital Image Processing, 2nd edition. ed. Prentice Hall, Upper Saddle River, N.J.

Grabner, G., Janke, A.L., Budge, M.M., Smith, D., Pruessner, J., Collins, D.L., 2006. Symmetric atlasing and model based segmentation: an application to the hippocampus in older adults. Med. Image Comput. Comput.-Assist. Interv. MICCAI Int. Conf. Med. Image Comput. Comput.-Assist. Interv. 9, 58–66.

Grossman, N., Bono, D., Dedic, N., Kodandaramaiah, S.B., Rudenko, A., Suk, H.-J., Cassara, A.M., Neufeld, E., Kuster, N., Tsai, L.-H., Pascual-Leone, A., Boyden, E.S., 2017. Noninvasive Deep Brain Stimulation via Temporally Interfering Electric Fields. Cell 169, 1029-1041.e16. https://doi.org/10.1016/j.cell.2017.05.024

Guler, S., Dannhauer, M., Erem, B., Macleod, R., Tucker, D., Turovets, S., Luu, P., Erdogmus, D., Brooks, D.H., 2016. Optimization of focality and direction in dense electrode array transcranial direct current stimulation (tDCS). J. Neural Eng. 13, 036020. https://doi.org/10.1088/1741-2560/13/3/036020

Hirata, A., Akazawa, Y., Kodera, S., Otsuru, N., Laakso, I., 2024. Electric Field Envelope Focality in Superficial Brain Areas with Linear Alignment Montage in Temporal Interference Stimulation. Comput. Biol. Med. 108697. https://doi.org/10.1016/j.compbiomed.2024.108697

Huang, Y., 2023. Visualizing interferential stimulation of human brains. Front. Hum. Neurosci. 17.

Huang, Y., 2019. ROAST: A simulator for TES. Available at https://github.com/andypotatohy/roast.

Huang, Y., Datta, A., 2021. Comparison of optimized interferential stimulation using two pairs of electrodes and two arrays of electrodes, in: 2021 43rd Annual International Conference of the IEEE Engineering in Medicine & Biology Society (EMBC). Presented at the 2021

43rd Annual International Conference of the IEEE Engineering in Medicine & Biology Society (EMBC), pp. 4180–4183. https://doi.org/10.1109/EMBC46164.2021.9631012
Huang, Y., Datta, A., Bikson, M., Parra, L.C., 2019. Realistic volumetric-approach to simulate transcranial electric stimulation—ROAST—a fully automated open-source pipeline. J. Neural Eng. 16, 056006. https://doi.org/10.1088/1741-2552/ab208d
Huang, Y., Datta, A., Parra, L.C., 2020. Optimization of interferential stimulation of the human brain with electrode arrays. J. Neural Eng. 17, 036023. https://doi.org/10.1088/1741-2552/ab92b3
Huang, Y., Liu, A.A., Lafon, B., Friedman, D., Dayan, M., Wang, X., Bikson, M., Doyle, W.K., Devinsky, O., Parra, L.C., 2017. Measurements and models of electric fields in the in vivo human brain during transcranial electric stimulation. eLife 6, e18834. https://doi.org/10.7554/eLife.18834
Huang, Y., Parra, L.C., 2019. Can transcranial electric stimulation with multiple electrodes reach deep targets? Brain Stimulat. 12, 30–40. https://doi.org/10.1016/j.brs.2018.09.010
Huang, Y., Thomas, C., Datta, A., Parra, L.C., 2018. Optimized tDCS for Targeting Multiple Brain Regions: An Integrated Implementation, in: 2018 40th Annual International Conference of the IEEE Engineering in Medicine and Biology Society (EMBC). Presented at the 2018 40th Annual International Conference of the IEEE Engineering in Medicine and Biology Society (EMBC), pp. 3545–3548. https://doi.org/10.1109/EMBC.2018.8513034
Iszak, K., Gronemann, S.M., Meyer, S., Hunold, A., Zschüntzsch, J., Bähr, M., Paulus, W., Antal, A., 2023. Why Temporal Inference Stimulation May Fail in the Human Brain: A Pilot Research Study. Biomedicines 11, 1813. https://doi.org/10.3390/biomedicines11071813
Kemether, E.M., Buchsbaum, M.S., Byne, W., Hazlett, E.A., Haznedar, M., Brickman, A.M., Platholi, J., Bloom, R., 2003. Magnetic resonance imaging of mediodorsal, pulvinar, and centromedian nuclei of the thalamus in patients with schizophrenia. Arch. Gen. Psychiatry 60, 983–991. https://doi.org/10.1001/archpsyc.60.9.983
Klem, G.H., Lüders, H.O., Jasper, H.H., Elger, C., 1999. The ten-twenty electrode system of the International Federation. The International Federation of Clinical Neurophysiology. Electroencephalogr. Clin. Neurophysiol. Suppl. 52, 3–6.
Lee, S., Lee, C., Park, J., Im, C.-H., 2020. Individually customized transcranial temporal interference stimulation for focused modulation of deep brain structures: a simulation study with different head models. Sci. Rep. 10, 11730. https://doi.org/10.1038/s41598-020-68660-5
Lee, S., Park, J., Choi, D.S., Lee, C., Im, C.-H., 2022. Multipair transcranial temporal interference stimulation for improved focalized stimulation of deep brain regions: A simulation study. Comput. Biol. Med. 143, 105337. https://doi.org/10.1016/j.compbiomed.2022.105337
Meinzer, M., Darkow, R., Lindenberg, R., Flöel, A., 2016. Electrical stimulation of the motor cortex enhances treatment outcome in post-stroke aphasia. Brain 139, 1152–1163. https://doi.org/10.1093/brain/aww002
Mirzakhalili, E., Barra, B., Capogrosso, M., Lempka, S.F., 2020. Biophysics of Temporal Interference Stimulation. Cell Syst. 11, 557-572.e5. https://doi.org/10.1016/j.cels.2020.10.004
Nitsche, M.A., Paulus, W., 2000. Excitability Changes Induced in the Human Motor Cortex by Weak Transcranial Direct Current Stimulation. J. Physiol. 527, 633–639. https://doi.org/10.1111/j.1469-7793.2000.t01-1-00633.x
Rampersad, S., Roig-Solvas, B., Yarossi, M., Kulkarni, P.P., Santarnecchi, E., Dorval, A.D., Brooks, D.H., 2019. Prospects for transcranial temporal interference stimulation in humans: A computational study. NeuroImage 202, 116124. https://doi.org/10.1016/j.neuroimage.2019.116124
Ruffini, G., Fox, M.D., Ripolles, O., Miranda, P.C., Pascual-Leone, A., 2014. Optimization of

multifocal transcranial current stimulation for weighted cortical pattern targeting from realistic modeling of electric fields. NeuroImage 89, 216–225. https://doi.org/10.1016/j.neuroimage.2013.12.002

Sadleir, R.J., Vannorsdall, T.D., Schretlen, D.J., Gordon, B., 2012. Target Optimization in Transcranial Direct Current Stimulation. Front. Psychiatry 3. https://doi.org/10.3389/fpsyt.2012.00090

Thiele, C., Rufener, K.S., Repplinger, S., Zaehle, T., Ruhnau, P., 2024. Transcranial temporal interference stimulation (tTIS) influences event-related alpha activity during mental rotation. Psychophysiology 61, e14651. https://doi.org/10.1111/psyp.14651

Van Essen, D.C., Ugurbil, K., Auerbach, E., Barch, D., Behrens, T.E.J., Bucholz, R., Chang, A., Chen, L., Corbetta, M., Curtiss, S.W., Della Penna, S., Feinberg, D., Glasser, M.F., Harel, N., Heath, A.C., Larson-Prior, L., Marcus, D., Michalareas, G., Moeller, S., Oostenveld, R., Petersen, S.E., Prior, F., Schlaggar, B.L., Smith, S.M., Snyder, A.Z., Xu, J., Yacoub, E., WU-Minn HCP Consortium, 2012. The Human Connectome Project: a data acquisition perspective. NeuroImage 62, 2222–2231. https://doi.org/10.1016/j.neuroimage.2012.02.018

Vassiliadis, P., Stiennon, E., Windel, F., Wessel, M.J., Beanato, E., Hummel, F.C., 2024. Safety, tolerability and blinding efficiency of non-invasive deep transcranial temporal interference stimulation: first experience from more than 250 sessions. J. Neural Eng. https://doi.org/10.1088/1741-2552/ad2d32

Violante, I.R., Alania, K., Cassarà, A.M., Neufeld, E., Acerbo, E., Carron, R., Williamson, A., Kurtin, D.L., Rhodes, E., Hampshire, A., Kuster, N., Boyden, E.S., Pascual-Leone, A., Grossman, N., 2023. Non-invasive temporal interference electrical stimulation of the human hippocampus. Nat. Neurosci. 1–11. https://doi.org/10.1038/s41593-023-01456-8

von Conta, J., Kasten, F.H., Ćurčić-Blake, B., Aleman, A., Thielscher, A., Herrmann, C.S., 2021. Interindividual variability of electric fields during transcranial temporal interference stimulation (tTIS). Sci. Rep. 11, 20357. https://doi.org/10.1038/s41598-021-99749-0

von Conta, J., Kasten, F.H., Schellhorn, K., Ćurčić-Blake, B., Aleman, A., Herrmann, C.S., 2022. Benchmarking the effects of transcranial temporal interference stimulation (tTIS) in humans. Cortex 154, 299–310. https://doi.org/10.1016/j.cortex.2022.05.017

Xiao, Q., Zhong, Z., Lai, X., Qin, H., 2019. A multiple modulation synthesis method with high spatial resolution for noninvasive neurostimulation. PLOS ONE 14, e0218293. https://doi.org/10.1371/journal.pone.0218293

Yatsuda, K., Yu, W., Gomez-Tames, J., 2024. Population-level insights into temporal interference for focused deep brain neuromodulation. Front. Hum. Neurosci. 18. https://doi.org/10.3389/fnhum.2024.1308549

Zhang, Y., Zhou, Z., Zhou, J., Qian, Z., Lü, J., Li, L., Liu, Y., 2022. Temporal interference stimulation targeting right frontoparietal areas enhances working memory in healthy individuals. Front. Hum. Neurosci. 16. https://doi.org/10.3389/fnhum.2022.918470

Figure captions

Fig. 1: Topoplots of optimized montages targeting the right hippocampus for HD-TES (left column), 2-array TI (middle column), and 2-pair TI (right column). Here only the montages for the first five subjects are shown (rows A–E, respectively). For TI, the two topoplots at each panel show the montages for the two frequencies.

Fig. 2: Topoplots of standard deviation across the ten subjects of the injected current at each electrode, for HD-TES (left column), 2-array TI (middle column), and 2-pair TI (right column), in targeting the right hippocampus (row A), the left DLPFC (row B), and the left motor cortex (row C). For TI, the two topoplots at each panel show the standard deviation for the two frequencies.

Fig. 3: Focality-modulation curves for the ten subjects targeting the right hippocampus (A1), the left DLPFC (A2), and the left motor cortex (A3), under 12 different levels of energy constraints for the non-target area. Different colors represent different subjects, with solid lines representing 2-array TI and dashed lines representing HD-TES. Normalized curves are shown in panels B1–B3, where modulation depth was normalized between 0% and 100%. Solid lines and shaded areas represent the mean and standard deviation of the focality measures (in centimeter) across subjects, with red and blue indicating 2-array TI and HD-TES, respectively.

Fig. 4: Examples of optimized montages and the corresponding distributions of modulation depth for targeting the right hippocampus (A1–A7), the left DLPFC (B1--B7), and the left motor cortex (C1–C7). Panels to the left of the vertical divider show results from optimized HD-TES, while panels to the right of the divider show optimized 2-array TI. For TI, the two topoplots show the montages for the two frequencies. Modulation depth (MD) and the focality of the MD at the target are noted.

Fig. 5: Focality-modulation curves for the ten subjects targeting using HD-TES the right hippocampus (A1), the left DLPFC (A2), and the left motor cortex (A3), under 12 different levels of energy constraints for the non-target area. Different colors represent different subjects, with solid lines representing results using individually optimized montages and dashed lines results using a common montage obtained from targeting on the standard MNI152 head. Normalized curves are shown in panels B1–B3, where modulation depth was normalized between 0% and 100%. Solid lines and shaded areas represent the mean and standard deviation of the focality measures (in centimeter) across subjects, with red and blue indicating optimized and common montages, respectively.

Fig. 6: Similar to Fig. 5, but for 2-array TI.

Fig. 7: Similar to Fig. 5, but for 2-pair TI. Note there is no energy constraint explicitly specified in optimizing TI using two pairs of electrodes, and thus the results are shown in points instead of curves. Different colors represent different subjects.

Fig 8: Examples of montages and the corresponding distributions of modulation depth for HD-TES (A1–A6), 2-array TI (B1--B8), and 2-pair TI (C1–C8). Panels to the left of the vertical divider show results from using a common montage obtained from targeting the right hippocampus on the standard MNI152 head, while panels to the right of the divider show results from using individually optimized montages targeting the right hippocampus. For TI, the two

topoplots show the montages for the two frequencies. Modulation depth (MD) and the focality of the MD at the target are noted.

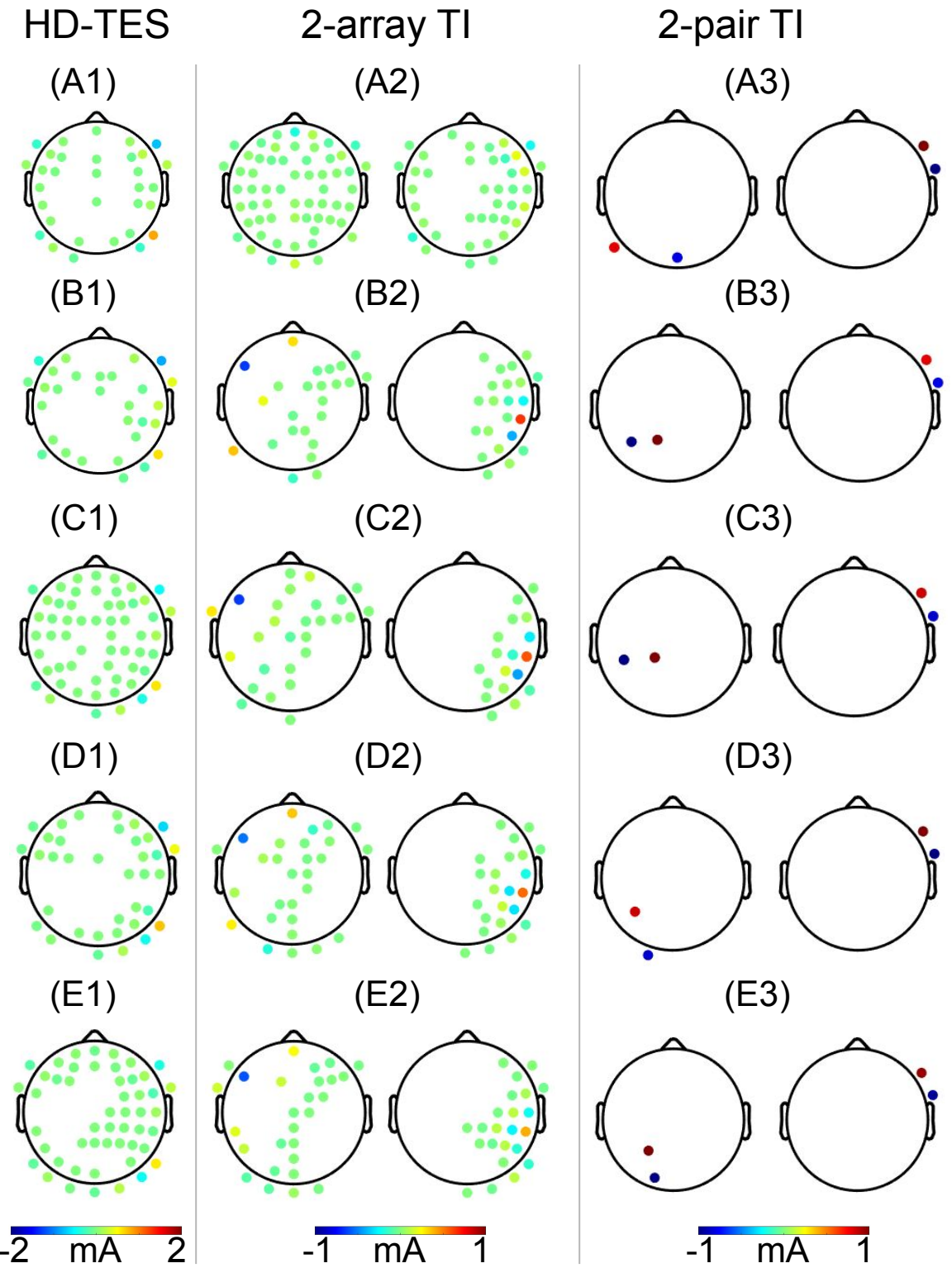
HD-TES
2-array TI
2-pair TI
(A1)
(A2)
(A3)
(B1)
(B2)
(B3)
(C1)
(C2)
(C3)
(D1)
(D2)
(D3)
(E1)
(E2)
(E3)
-2 mA 2
-1 mA 1
-1 mA 1

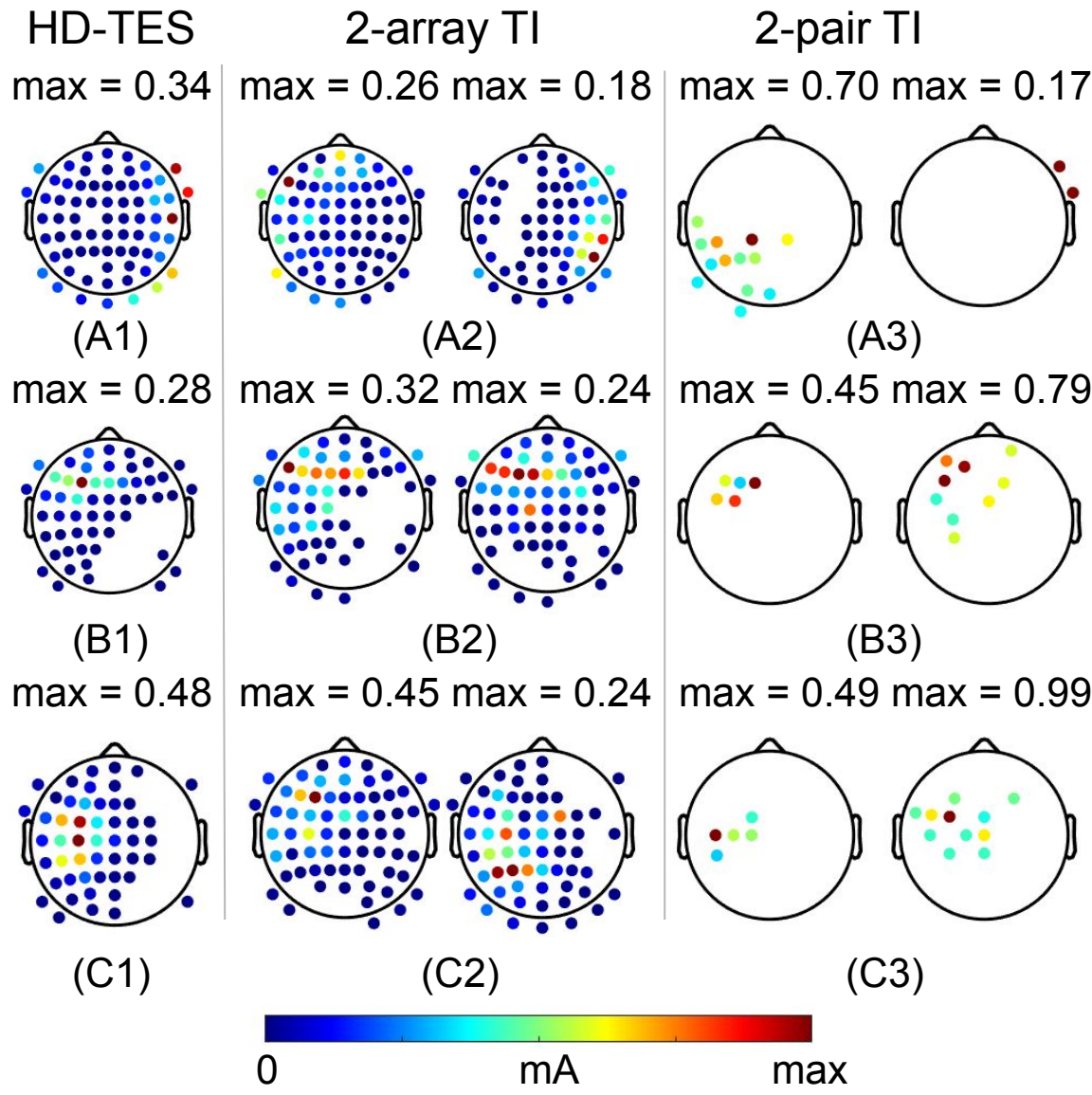
HD-TES
2-array TI
2-pair TI
max = 0.34
max = 0.26 max = 0.18
max = 0.70 max = 0.17
(A1)
(A2)
(A3)
max = 0.28
max = 0.32 max = 0.24
max = 0.45 max = 0.79
(B1)
(B2)
(B3)
max = 0.48
max = 0.45 max = 0.24
max = 0.49 max = 0.99
(C1)
(C2)
(C3)
0
mA
max

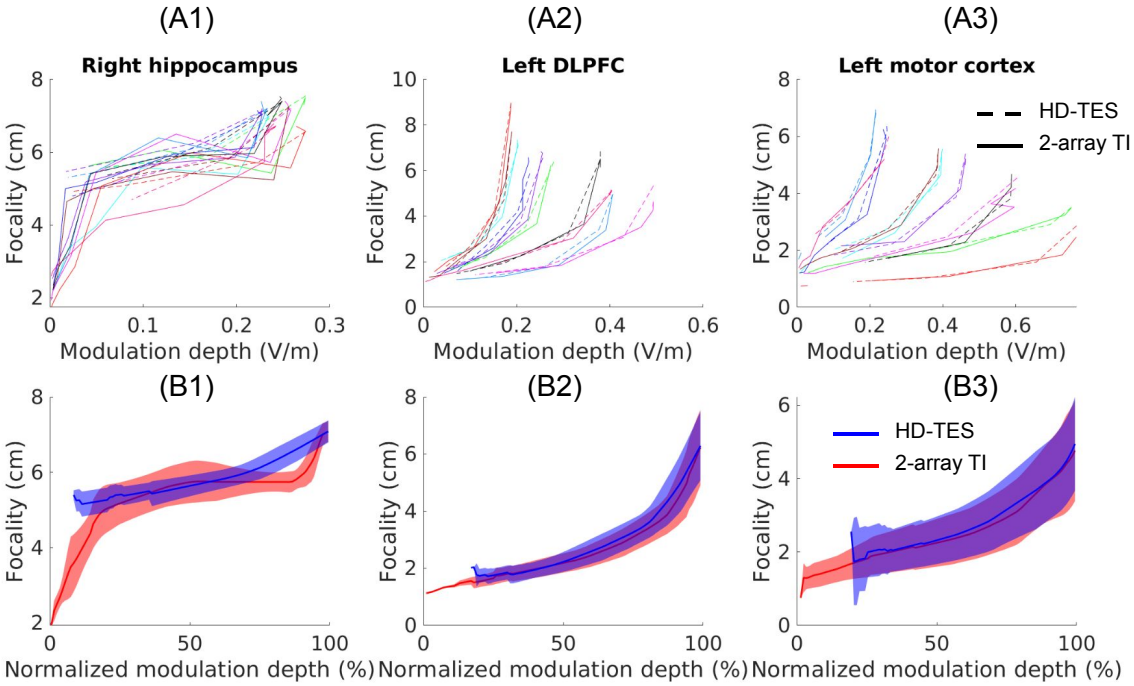
(A1)
Right hippocampus
Focality (cm)
Modulation depth (V/m)
(A2)
Left DLPFC
Focality (cm)
Modulation depth (V/m)
(A3)
Left motor cortex
HD-TES
2-array TI
Focality (cm)
Modulation depth (V/m)
(B1)
Focality (cm)
Normalized modulation depth (%)
(B2)
Focality (cm)
Normalized modulation depth (%)
(B3)
HD-TES
2-array TI
Focality (cm)
Normalized modulation depth (%)

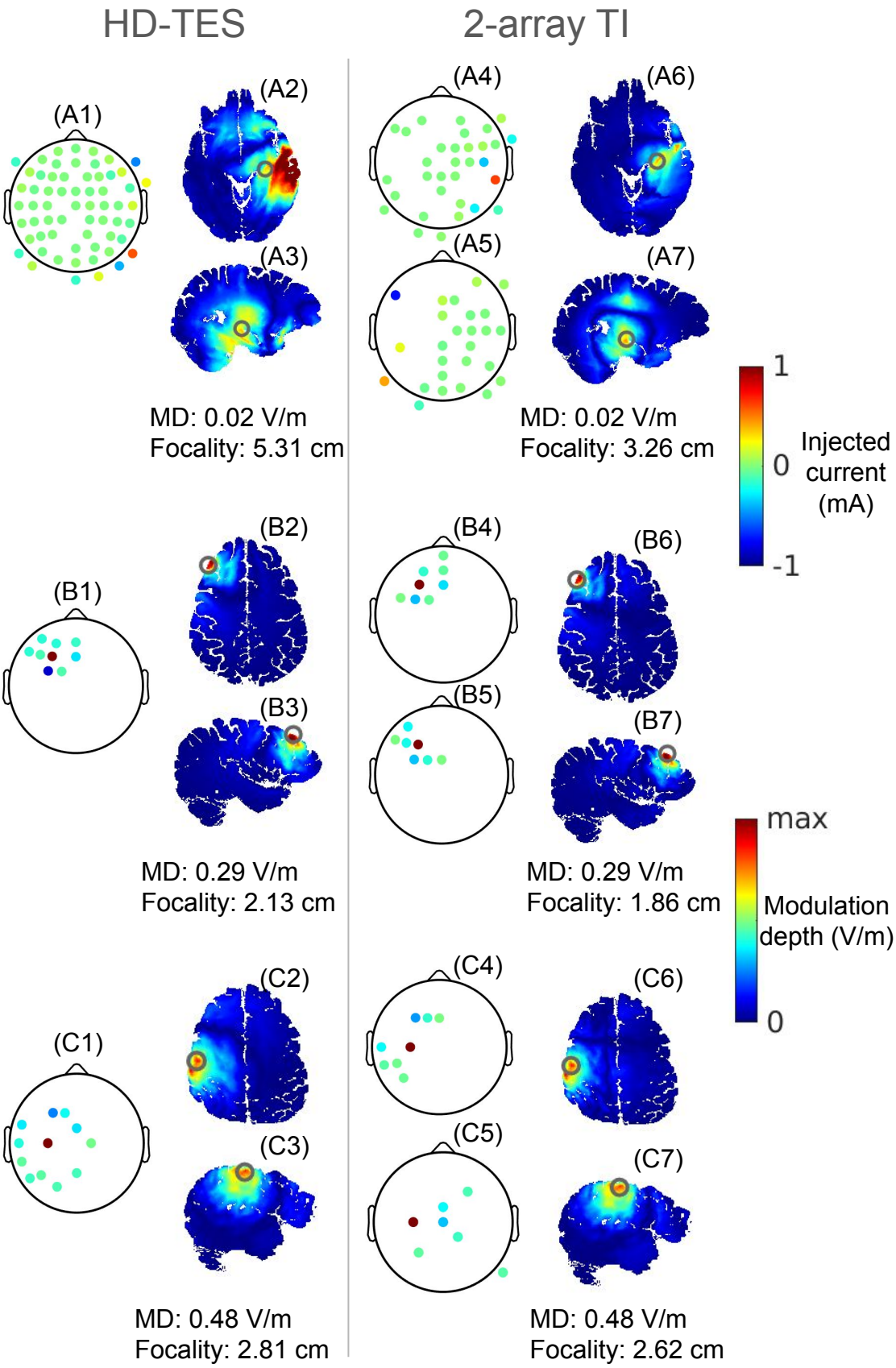
HD-TES
2-array TI
(A1)
(A2)
(A3)
MD: 0.02 V/m
Focality: 5.31 cm
(A4)
(A5)
(A6)
(A7)
MD: 0.02 V/m
Focality: 3.26 cm
1
0
-1
Injected current (mA)
(B1)
(B2)
(B3)
MD: 0.29 V/m
Focality: 2.13 cm
(B4)
(B5)
(B6)
(B7)
MD: 0.29 V/m
Focality: 1.86 cm
max
Modulation depth (V/m)
0
(C1)
(C2)
(C3)
MD: 0.48 V/m
Focality: 2.81 cm
(C4)
(C5)
(C6)
(C7)
MD: 0.48 V/m
Focality: 2.62 cm

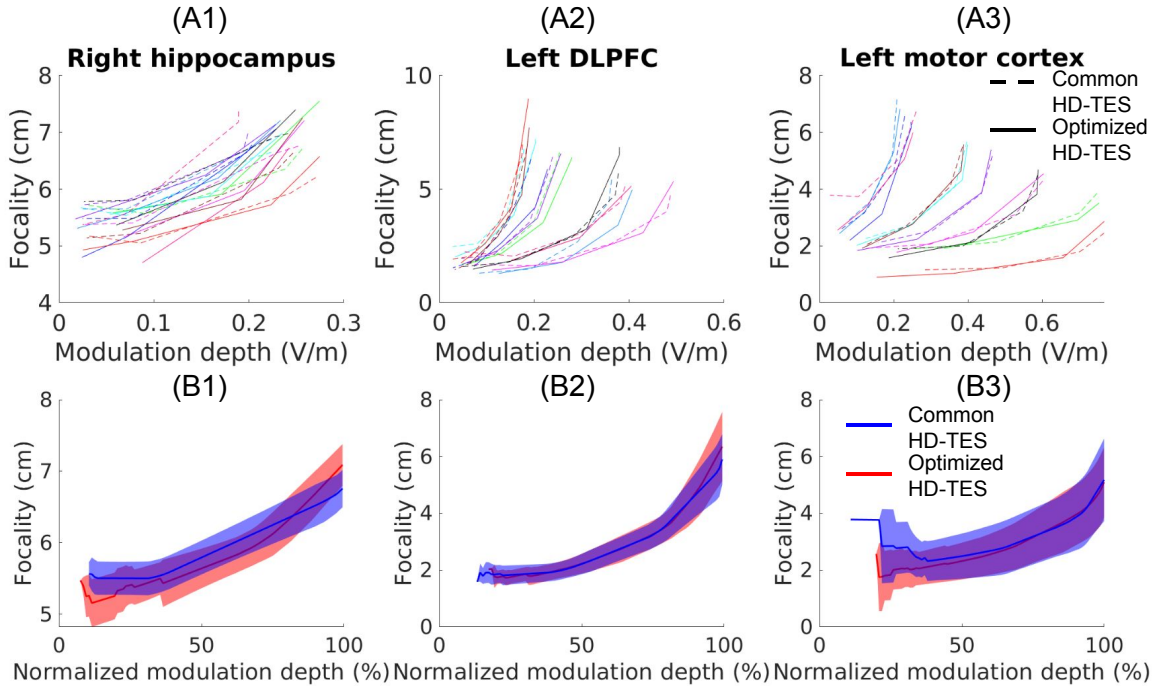
(A1)
Right hippocampus
(A2)
Left DLPFC
(A3)
Left motor cortex
Common HD-TES
Optimized HD-TES
Focality (cm)
Modulation depth (V/m)
(B1)
(B2)
(B3)
Normalized modulation depth (%)

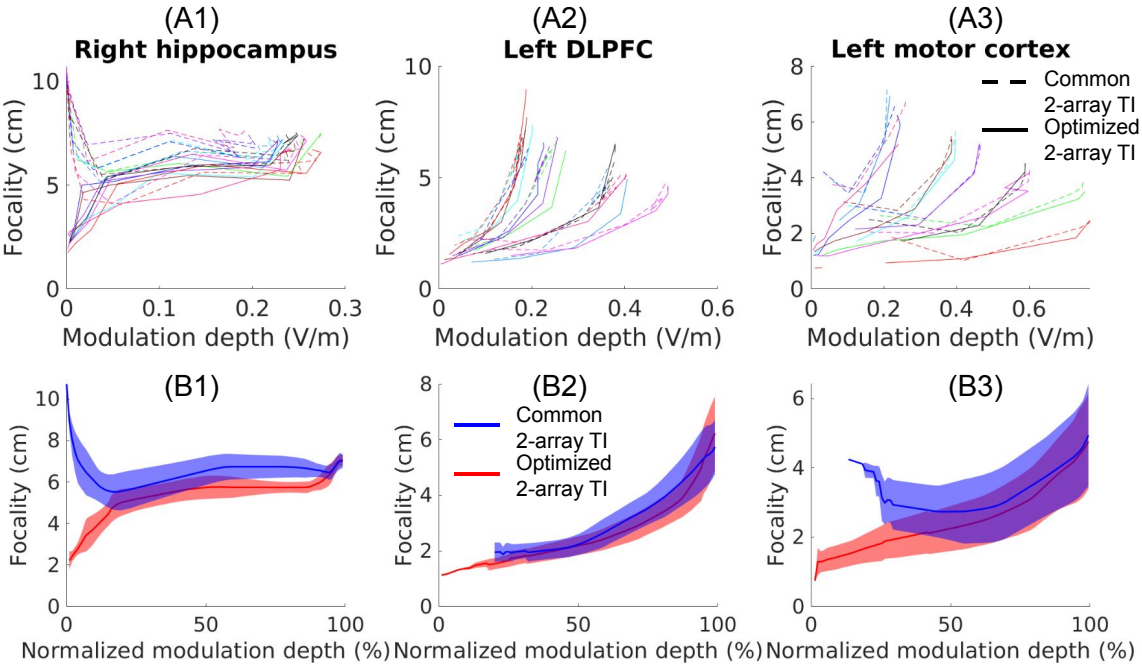
(A1)
Right hippocampus
(A2)
Left DLPFC
(A3)
Left motor cortex
Common 2-array TI
Optimized 2-array TI
Focality (cm)
Modulation depth (V/m)
(B1)
(B2)
(B3)
Normalized modulation depth (%)

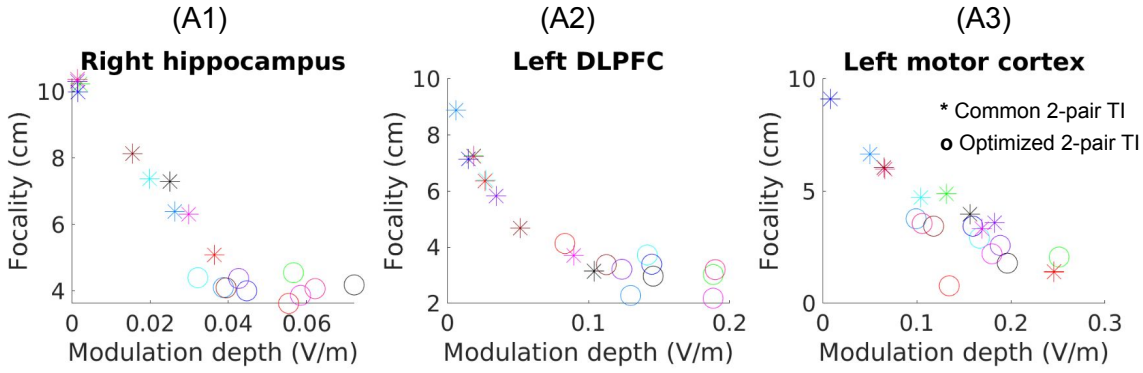
(A1)
Right hippocampus
Focality (cm)
Modulation depth (V/m)
(A2)
Left DLPFC
Focality (cm)
Modulation depth (V/m)
(A3)
Left motor cortex
Focality (cm)
Modulation depth (V/m)
* Common 2-pair TI
o Optimized 2-pair TI

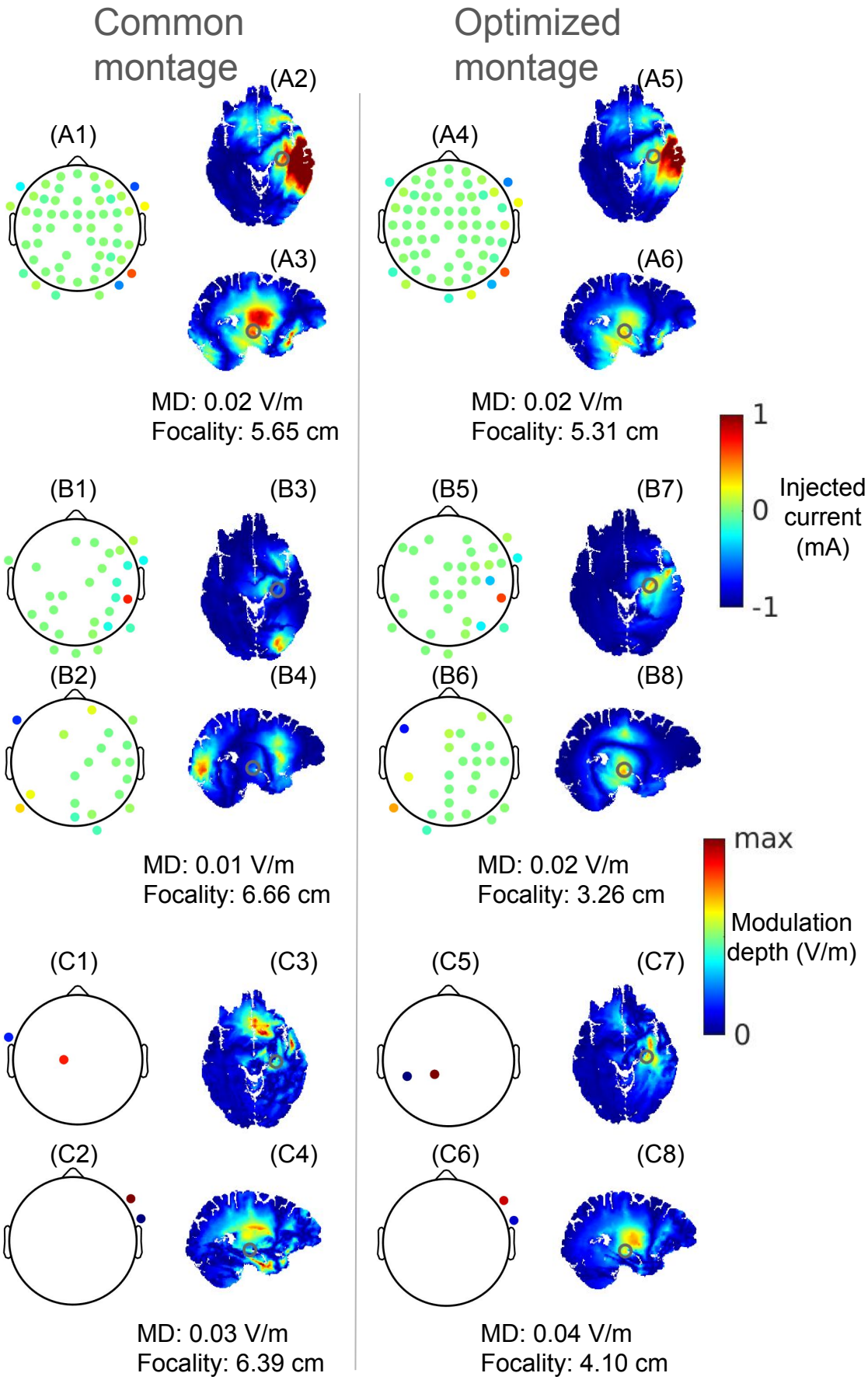
Common montage
Optimized montage
(A1)
(A2)
(A3)
(A4)
(A5)
(A6)
MD: 0.02 V/m
Focality: 5.65 cm
MD: 0.02 V/m
Focality: 5.31 cm
1
0
-1
Injected current (mA)
(B1)
(B2)
(B3)
(B4)
(B5)
(B6)
(B7)
(B8)
MD: 0.01 V/m
Focality: 6.66 cm
MD: 0.02 V/m
Focality: 3.26 cm
max
Modulation depth (V/m)
0
(C1)
(C2)
(C3)
(C4)
(C5)
(C6)
(C7)
(C8)
MD: 0.03 V/m
Focality: 6.39 cm
MD: 0.04 V/m
Focality: 4.10 cm